Title

Laser-transected microtubules exhibit individuality of regrowth, however most free new ends of the microtubules are stable.

Journal

Journal of Cell Biology, 107(3)

ISSN

0021-9525

Authors

Tao, W

Walter, RJ

Berns, MW

Publication Date

1988-09-01

DOI

10.1083/jcb.107.3.1025

Laser-transected Microtubules Exhibit Individuality of Regrowth, However Most Free New Ends of the Microtubules Are Stable

Wen Tao, Robert J. Walter, and Michael W. Berns

Beckman Laser Institute and Medical Clinic, University of California at Irvine, Irvine, California 92717

Abstract. To study the possible mechanism of microtubule turnover in interphase cells, we have used the 266-nm wavelength of a short-pulsed Nd/YAG laser to transect microtubules in situ in PtK_2 cells at predefined regions. The regrowth and shrinkage of the transected microtubules have been examined by staining the treated cells with antitubulin mAb at various time points after laser irradiation. The results demonstrate that microtubules grow back into the transected zones individually; neither simultaneous growth nor shrinkage of all microtubules has been observed. The half-time of replacement of laser-dissociated microtubules is observed to be ~10 min. On the other hand, exposure of the core of the microtubule, which is expected to consist almost completely of GDP-tubulin, by transecting the internal regions of the microtubule does not render the remaining polymer catastrophically disassembled, and most transected microtubules with free minus ends do not quickly disappear. Taken together, these results suggest that most microtubules in cultured interphase cells exhibit some properties of dynamic instability (individual regrowth or shrinkage); however, other factors in addition to the hydrolysis of GTP-tubulin need to be involved in modulating the dynamics and the stability of these cytoplasmic microtubules.

MICROTUBULES (MTs)[1] are one of the three major fibrillar systems of the cytoskeleton and play an important role in cell movement, determination of cell shape, organization of the internal architecture of the cell, and segregation of chromosomes in mitosis (10, 34). For a better understanding of these fundamental cellular processes it is essential to understand the mechanism of assembly of the MT polymer.

MTs were initially postulated to be polymers in a simple equilibrium with the free tubulin subunits (18, 30). Subsequently, evidence indicated that this view was overly simple. Experimental as well as theoretical explorations of the role of nucleotide hydrolysis in assembly led to the treadmilling model which proposes that, at steady state, there may be a net tubulin addition at one end of the polymer and a net loss from the other end, resulting in a unidirectional flux of tubulin through MTs (9, 25; reviewed in reference 26). More recently, based on observations of individual MT behavior under conditions in which the free monomer concentration is equal to or below the steady-state concentration and on modeling of dynamics of theoretical MTs using hypothetical values for the rate constants, an alternative "dynamic instability" model was proposed. This model asserts that over a wide tubulin concentration range, a slow growing phase and rapid shrinking phase may coexist in a population of MTs; growing MTs are postulated to have tubulin subunits with bound GTP at the polymer ends, while the terminal subunits in shrinking MTs are thought to have bound GDP. The two phases interconvert stochastically and infrequently (15, 16, 23, 27, 28).

At present, it appears that more is known about the assembly of tubulin dimers into MTs under various artificial conditions in vitro than in living cells. Microinjection of fluorescently labeled tubulin into living cells and subsequent immunocytochemistry or measurement of fluorescence redistribution after laser photobleaching has demonstrated that intracellular MTs must be in a dynamic steady state (5, 36, 38, 40), although the mechanism of MT assembly in cells is not well understood. One recent study suggested that dynamic instability may be the mechanism of MT turnover in living fibroblasts; however, the lack of overall high resolution of individual MTs made the interpretation of the experiments difficult (37). There are several other possible drawbacks associated with microinjection experiments: an increase in intracellular tubulin concentration and in total cell volume, mixture of labeled and endogenous tubulins, and differences of behavior between the labeled and unmodified subunits.

Selective subcellular microsurgery on many cell structures using a variety of focused laser beams has been well developed (reviewed in reference 2). Furthermore, it has been shown that a short-pulsed UV laser can be used to ablate an

1. *Abbreviation used in this paper*: MT, microtubule.

organic polymer or biological tissue with no detectable thermal damage to the substrate (41).

We have combined the techniques of laser microsurgery and immunocytochemistry, and designed a series of experiments to examine the mechanism of assembly and disassembly of cytoplasmic MTs in interphase cells. The results show that MTs grow back into the transected zones individually after laser transection. The half-time of MT replacement was observed to be ~10 min. The simultaneous growth or shrinkage of all transected MTs predicted by the treadmilling model was never observed under the experimental conditions. This suggests that the majority of cytoplasmic MTs exhibit some properties of dynamic instability. But most transected MTs with free new ends generated by laser irradiation do not immediately disassemble to completion, and the free minus ends of these MTs are relatively stable for a period of >10 min. This suggests that the presence of other factors besides the hydrolysis of GTP-tubulin modulates the dynamics and stability of the cytoplasmic MTs.

Materials and Methods

Cell Culture

PtK_2 cells (rat kangaroo kidney epithelium) were originally obtained from the American Type Culture Collection (ATCC; Rockville, MD), and have the advantage in that they are thin and remain relatively flat throughout their cell cycle. The cells were grown as monolayers in minimal essential medium (Gibco Laboratories, Grand Island, NY) containing 10% FCS without antibiotics. Cultures were maintained at 37°C in a humidified atmosphere of 5% CO_2.

Laser Transection of MTs

The laser microbeam system was similar to that described previously (42). Laser transection of MTs was performed on cells in Rose culture chambers using the fourth harmonic 266-nm wavelength from a short-pulsed Nd/YAG laser (model YG 481A; Quantel Corp., Tempe, AZ). The pulse energy of the unfocused laser beam was found to be 63–144 microjoules before attenuation, with a pulse duration of 10 ns. Laser energy was controlled with neutral density filters (Oriel Corp. of America, Stanford, CT) placed in the light path. For each individual experiment, the laser pulse energy was carefully monitored and controlled so that it remained constant throughout the experiment. The laser was diverted by a series of optical mirrors and a dichroic filter into an inverted Axomat microscope (Carl Zeiss, Inc., Thornwood, NY), and focused through a 100× Ultrafluar objective (Carl Zeiss, Inc.). The effective spot size of the focused laser beam was estimated to be 5 μm in diameter. Frequency of the pulses was controlled by an electronic shutter synchronized with the laser.

The cells were seeded in Rose culture chambers with quartz coverslips, as one chamber window, 36–40 h before the experiments. To minimize cell-to-cell variability, the cells with a similar size (~100 μm long) and elliptic shape were selected for this study. The positions of the selected cells were marked by scribing small circles (1.0 mm in diameter) around them on the outside surface of the quartz coverslips using a diamond marking objective. Observation of the target cells and accurate determination of predefined regions were accomplished by projecting the cell images, through a Newvicon tube video camera (Sierra Scientific Corp., Mountain View, CA), onto a video monitor interfaced with an image array processor, and superimposing a rectangular cursor box at a preselected area on the real-time image of a cell. Transection of cytoplasmic MTs was achieved by moving the xy motorized stage with a joystick controller so that the focused laser beam raster-scanned in straight lines through the entire cursor box–outlined cytoplasm of a target cell. The scan lines were parallel to the long axis of the cursor box. On average, it took ~8 s to transect MTs and produce a transected zone in a given cell. The predefined regions were always 19–23 μm away from the leading edges of the cells and had a width of 5 μm across the cells. For each experiment, several cells in a Rose chamber were selected, marked, and MTs in the transected zones within these cells were dissociated at various time points by the laser as described above. The microscope stage was kept at 37°C using an air curtain incubator. Photographs were taken before and after irradiation. After treatment of the last selected cell, the cells were immediately fixed and then processed for immunofluorescence.

Immunofluorescence

About 20 s after the last laser transection, the cells were fixed for 10 min in 3.7% formaldehyde in PBS with three changes by injecting the fixative into the Rose chambers. The Rose chambers were then disassembled; the cells on the quartz coverslips were permeabilized for 1 min in 0.1% Triton X-100 in PBS, further fixed for 30 min with the same fixative, and extracted again for 15 min in 0.1% Triton X-100 in PBS. This treatment not only rapidly fixed the cells, resulting in good preservation of MTs, but also gave very good permeabilization. The fixed and permeabilized cells were incubated for 1 h at 37°C with anti-α-tubulin mAb (Amersham Corp., Arlington Heights, IL) diluted 1:100 in PBS. The cells were then freed of excess primary antibody by three washes with PBS and incubated for 30 min at 37°C with fluorescein-conjugated goat anti-mouse IgG+IgM (Boehringer Mannheim Biochemicals, Indianapolis, IN) diluted 1:70 in PBS. After fluorescent labeling, coverslips were washed in three changes of PBS for a total of 10 min, rinsed with double-distilled water, and mounted in Aquamount (Lerner Labs, New Haven, CT). Cells were subsequently examined with an epifluorescence microscope (Carl Zeiss Inc.) equipped with the appropriate excitation and barrier filters (Zeiss filter set No. 487710). All immunofluorescence micrographs were taken on Tri-X Pan film (Eastman Kodak Co., Rochester, NY) using 1-min exposures, and developed in Kodak Microdol-X.

Electron Microscopy

The cells were treated with the laser under the conditions identical to those described above. Immediately after the treatment, the cells were fixed for 10 min in 3% glutaraldehyde in medium, washed with PBS twice, and further fixed for another 50 min with the same fixative. Subsequently, the Rose chambers were disassembled, and the locations of the treated cells were marked using a diamond pen. Fixed cells on the quartz coverslips were washed twice with PBS, postfixed for 1 h with 1% osmium tetroxide in Millonig's phosphate buffer (pH 7.0), and rinsed in the same buffer. The cells were critical point dried after dehydration in a graded series of acetone (30–100%). Critical point–dried samples were then gold coated, and examined with a scanning EM (model SEM 515; Philips Electronic Instruments, Inc., Mahwah, NJ).

Viability Assay

Groups of cells in a Rose chamber were marked in 2-mm-diam circles as described. All cells inside the circles were treated with the laser under the same conditions described above. At various times after the treatment, the cells were rinsed with PBS and stained with 0.08% trypan blue in PBS for 10 min. The cells inside the circles were counted and the viability was expressed as the ratio of cells retaining the stain vs. total number of cells examined.

Data Analyses

The image processing system was described previously (44). For analyses, negatives were imaged with a Newvicon tube camera (model LST-1; Sierra Scientific Corp.); the images were digitized, processed with a Plessey 6200 computer system (Plessey Peripheral Systems, Irvine, CA) equipped with IP-512 image processing boards (Imaging Technology Inc., Woburn, CA), and displayed on a video monitor.

To determine accurately the location of transection on a phase-contrast or fluorescence micrograph, we collected an image from a phase-contrast or fluorescence micrograph, stored the image in the image processor, and subsequently superimposed it with another image of the same cell with the cursor box showing the predefined region.

Average gray value measurements were performed as follows. Images of fluorescence micrographs (negatives) were positioned in such a way that the longitudinal directions of transection aligned with the vertical axis of the video images. An interactive mouse-controlled cursor box, with the length corresponding to the length of the cell, was then displayed on the video monitor. The location and width of the cursor box was determined by the criteria that the cursor box should cover as much of the cellular region as possible while minimizing background regions. The average gray values within the

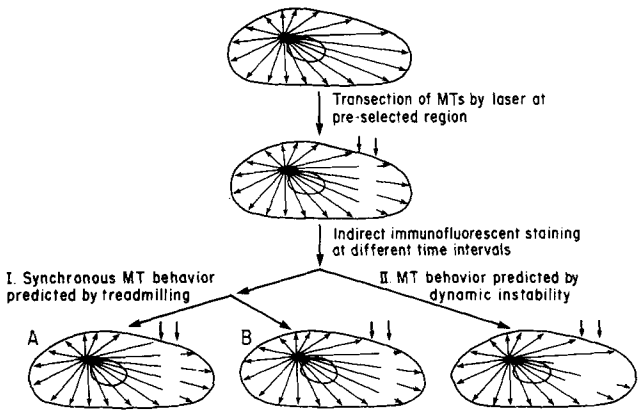

Figure 1. Schematic representation of the experimental design. Two arrows outside each cell indicate the transected zones within which MTs are dissociated by laser. MTs are depicted as lines inside the cells and the polarity of MTs is indicated by the arrows. See Results for details.

box were measured, integrated in a vertical direction, and displayed as a summed histogram showing the variation in average gray value vs. horizontal position in a cell. The displayed histograms were recorded on Kodak Panatomic-X film and traced onto transparent paper from enlarged prints made from the original negatives. The background average gray values were normalized with respect to those measured from a cell fixed 20 s after laser transection.

To quantitate MTs within the transected zones, we performed the following analysis. Micrographs (negatives) of tubulin-stained cells were imaged and processed as described, and the image contrast was optimized using system software. A mouse-controlled cursor box with a width of 10 μm and length corresponding to the width of the cell was then superimposed on the image to outline the transected zone; MTs within the cursor box were counted directly from the video monitor and calculated as MT density (number of MTs/500 μm^2). The surface area of 500 μm^2 was chosen because it was about the average of the surface areas of the cursor boxes. Quantification of MTs outside the transected zones was performed in the same way except that the cursor box was placed between the transected zones and the cell edges adjoining the transected zones.

Results

Experimental Design and Rationale

Most cytoplasmic MTs in tissue culture cells have been shown to originate from a centrosome or MT organizing center and to extend radially towards the cell periphery (31). Moreover, it is known that MT assembly both in living cells and in vitro experiments in crude lysates is initiated at the MT organizing center and that virtually all the MTs have the same polarity—their fast-growing ends distal to the site of initiation (1, 11, 14).

To test the possible models of MT assembly, we used a short-pulsed laser beam to transect MTs in situ in interphase PtK_2 cells at predefined regions followed by indirect immunofluorescent staining at various time points with antitubulin mAb to examine the behavior of transected MTs. Under these conditions, the treadmilling and dynamic instability models give distinct predictions with respect to the patterns of regrowth or shrinkage of the transected MTs. The rationale of the experiments is diagrammed in Fig. 1.

According to the treadmilling model, one would predict two different situations under steady-state conditions. In the first instance, if MTs are attached to a centrosome or a structural matrix by lateral linkages near their ends, in such a way that the ends remain free for subunit exchange (22, 26), the new plus end generated by transection would add subunits and the minus end at the centrosome would lose subunits at the same rate; similarly, the loss of subunits from the new minus end would be balanced by the addition of subunits from the plus end of the MT fragment. Therefore, the lengths of the MTs would not change and the transected zone would remain stationary with time (Fig. 1 *A*). Secondly, if the anchored minus ends of MTs are blocked by attaching to a centrosome (20), the new plus end would grow; but the loss of subunits from the new minus end would be balanced by the addition of subunits from the plus end. Thus, the transected zone would be filled in with time from the side in proximity to the centrosome (Fig. 1 *B*). In either case, the treadmilling model would predict synchronous behavior of MTs.

Under the experimental conditions, dynamic instability would predict that (*a*) MTs grow back into the transected zone individually—thus, the replacement of laser-dissociated MTs should occur MT by MT; and (*b*) the number of MTs found in the transected zone would increase gradually at certain time intervals after laser transection. Furthermore, the GTP cap model, which has been proposed as the mechanism of dynamic instability, would predict that transecting the internal regions of MTs would cause all the transected MTs with free exposed ends to be in the rapid-shrinking phase, and that a majority of these shrinking MTs would catastrophically depolymerize to completion since the phase transitions are expected to be low probability events (7, 16, 28). Therefore, according to the GTP cap model, one would expect a drastic decrease in the number of MTs in regions proximal from the transected zones in relation to the cell nuclei and almost complete lack of MTs in regions distal from the transected zones soon after laser transection.

Transection of Cytoplasmic MTs In Situ Using Laser at Accurately Predefined Regions

One of the prerequisites for our experiments is that there must be a means to transect MTs in living cells at desired regions which must be accurately relocated on subsequent analyses. To determine whether the short-pulsed UV laser can actually be used to dissociate MTs in a controlled manner, we focused the 266-nm wavelength of the short-pulsed Nd/YAG laser into the cytoplasm of interphase PtK_2 cells and manually raster-scanned the focused laser beam through the entire cytoplasmic area outlined by a superimposed cursor box as described in Materials and Methods. The computer-generated cursor box on a live video image of the living cell determined the scan zone. The cells were then fixed, and processed for immunofluorescence ~20 s after the laser treatment. The typical results (Fig. 2) show that the UV laser indeed could uniformly dissociate the cytoplasmic MTs in situ at selected regions and that such a transection is a localized reaction because the cytoplasmic regions outside the irradiated zone showed normal patterns of antitubulin labeling (Fig. 2 *c*). These observations have been confirmed using high voltage electron microscopy (Rieder, C. L., personal communication).

Surprisingly, the actual transected zone on the immunofluorescent image was ~10 μm in width, which was wider than the predefined region (Fig. 2 *c*). Such discrepancy is likely

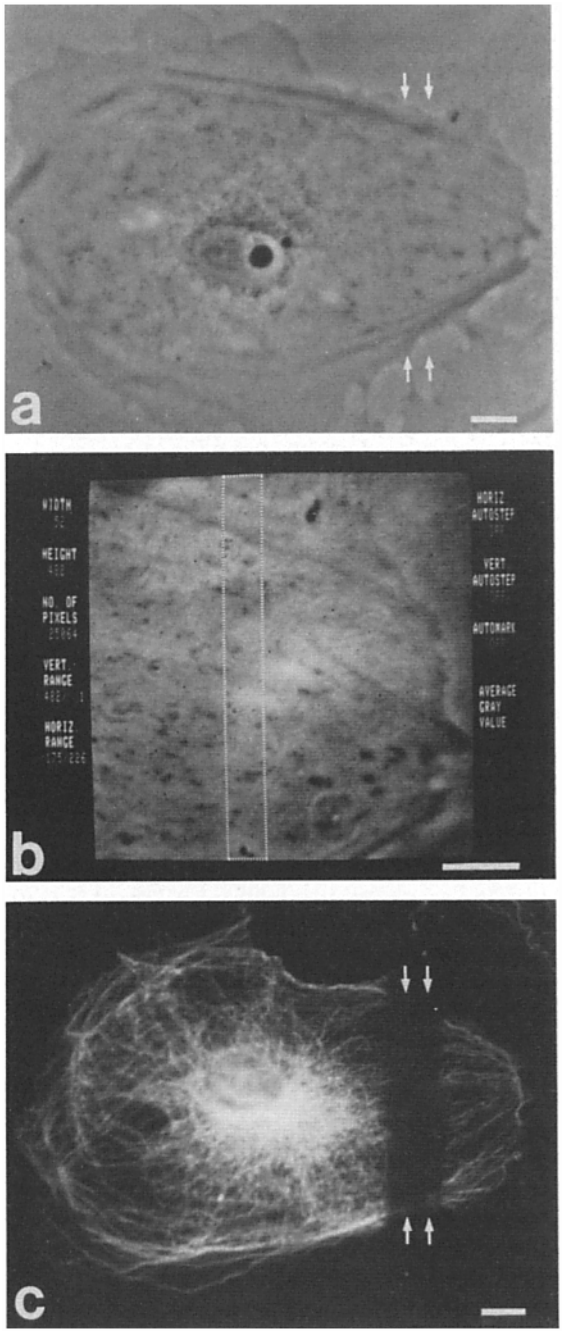

Figure 2. Local dissociation of cytoplasmic MTs by laser at predefined regions. (*a*) Phase-contrast image of an interphase PtK_2 cell. (*b*) Image of the same cell photographed from the video monitor showing that the predefined region is determined by the superimposed rectangular cursor box. (*c*) Corresponding tubulin staining of the same cell shows the lack of MTs in the transected zone and normal distribution of MTs elsewhere. *Arrows*, predefined regions. Bars, 10 μm.

due to the large effective spot size of the laser beam. This is inferred from the following facts. (*a*) The cells fixed 20, 40, and 50 s after laser transection under the identical conditions exhibited almost the same width of the transected zones. This argues against the possibility that the discrepancy could have resulted from the rapid transient depolymerization at the ends during the time interval between transection and fixation since it predicts that the widths of the transected zones would drastically vary with the time interval. (*b*) When the predefined region was narrowed, the width of the transected zone was observed to be proportionally reduced. (*c*) When a low magnification (32×) objective was used instead of the 100× objective, the widths of the transected zones were reduced, indicating that the aperture angles of the objectives play a role in determination of effective spot sizes of the laser microbeam.

Table I. Cell Viability after Laser Transection

Time after laser treatment	Cells stained	Cells treated	Survival rate
	n	*n*	%
20 s	1	172	99
	0	124	100
2 h	2	132	99
	0	107	100
4 h	0	118	100
	1	147	99
6 h	2	105	98
	1	131	99

Effects of Laser Irradiation on Cells

To estimate the effects of laser irradiation on cells other than on the cytoplasmic MTs, cell viability after laser treatment was assayed using the trypan blue dye exclusion method. The results (Table I) show that almost all the irradiated cells survived ≥6 h after irradiation.

Scanning EM on the treated cells was performed to determine whether laser irradiation might have damaged the cell membrane. The typical data (Fig. 3) reveal that there is no difference between the cell surface over the irradiated regions and that over control regions (Fig. 3, *b* and *c*). Therefore, to the limits of scanning EM, there is no detectable laser-induced damage to the cell membrane.

The effect of laser irradiation on cell morphology is shown in Fig. 4, *a* and *b*. The results demonstrate that laser transection of MTs did not induce remarkable changes in the overall cell morphology; however, some subtle morphological changes after irradiation did occur, as shown by changes in the phase-contrast images at the cell margins (*open arrows*, Fig. 4 *b*). Fig. 4 *c* reveals that the cytoplasmic MTs had indeed been transected and some of the MTs grew back into the transected zone since the cell was irradiated 10 min before fixation.

Furthermore, the laser-dissociated MTs were completely replaced by 40 min after laser irradiation (Figs. 5 and 7). Interestingly, a couple of cells were observed under the phase-contrast microscope to undergo mitosis within 1 h after laser irradiation. This indicates that the laser irradiation under the experimental conditions did not interfere with the cellular processes of transition from interphase to M phase (not shown). General observations of time-lapse video tape images of the cells after irradiation revealed normal-appearing cytoplasmic particle transport in nonirradiated regions (our unpublished data).

All these results strongly suggest that any possible pertur-

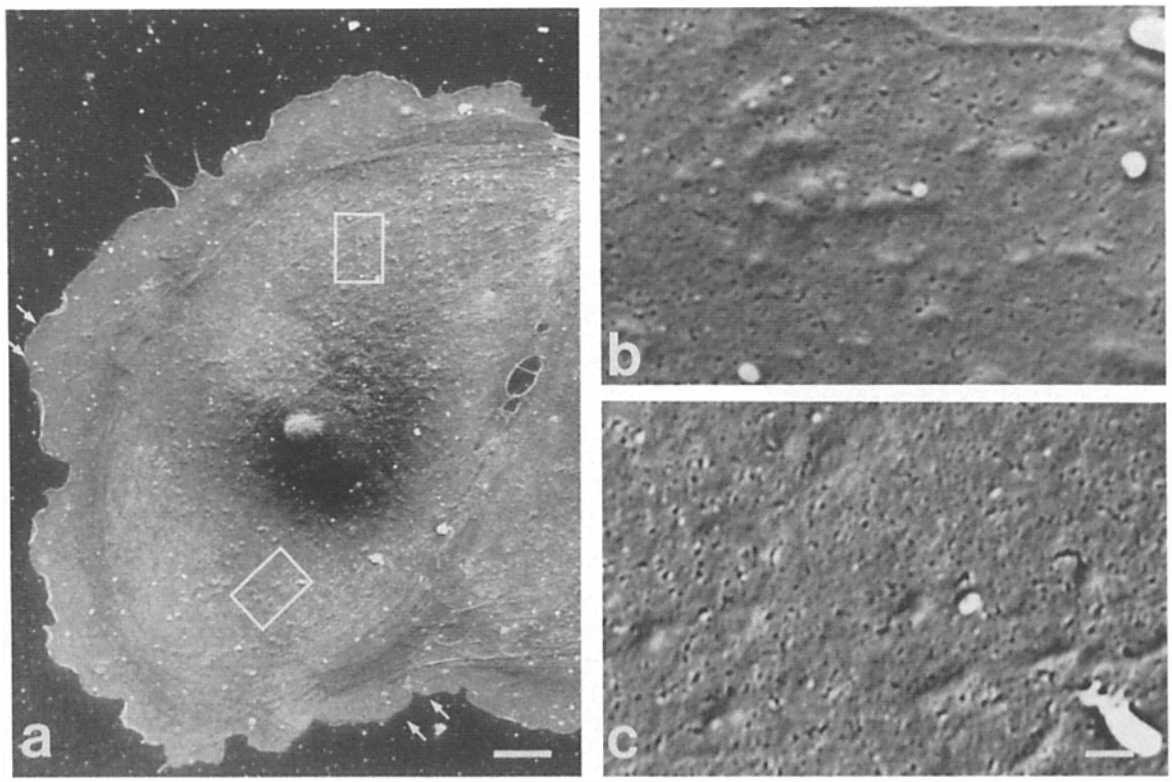

Figure 3. Scanning electron micrographs of a laser irradiated PtK_2 cell showing no detectable membrane damage. (*a*) Low magnification view of the PtK_2 cell in which the cytoplasmic MTs were dissociated using the laser at the region indicated by arrows. The upper and lower boxes in *a* indicate the boundaries of the field shown at higher magnification in *b* and *c*, respectively. (*b*) High magnification view of the cell surface at an untreated region. (*c*) High magnification view of the cell surface over the irradiated region. Bars: (*a*) 10 μm; (*b* and *c*) 1 μm.

bative effects of the laser irradiation on the cells is minimal under the experimental conditions used.

Replacement of Laser-dissociated MTs Occurs Individually with No Synchronous Behavior of MTs

To address the question whether the transected MTs behave individually or synchronously, we have fixed and stained the cells with monoclonal antitubulin at various time points after the laser transection of the cytoplasmic MTs. Representative results from such experiments are shown in Fig. 5. At 20 s after irradiation, the earliest time at which we are able to inject the fixative into the Rose culture chambers, we detect no MTs in transected zones with a width of ~10 μm, and the new MT ends created by transecting the internal regions of the MTs are evident (Figs. 2 and 5 *a*). The cells fixed 9, 13, and 19 min after laser transection (Fig. 5, *b–d*) show a progressive increase in the number of MTs in the transected zones, indicating that the transected and newly initiated MTs grow back into the transected zones individually. Some ends of the MTs can be easily seen in the area within or across the transected zones and in the area distant from the transected zones. Since all the free new MT ends produced by the transection were initially in line at the edges of the transected zone, we refer to the MTs with ends that lay within or across the transected zones as growing MTs, and to MTs with ends that lay distant from the transected zones as shrinking MTs. The growing and shrinking MTs can be found from both sides of the transected zones. At 28 and 35 min after laser transection, almost all the MT-depleted zones are replaced by newly grown MTs and the ends of the MTs near the transected zones can only be seen occasionally (Fig. 5, *e* and *f*). By 55 min after the transection, there is no difference between the MT distribution of treated cells and those of control cells (Fig. 5 *g*).

To determine the average properties of the regrowth or shrinkage of transected MTs, we have used computerized image analysis to measure the average gray values in digitized tubulin-stained images. In any given cell, the average density of tubulin staining should be proportional to the average number of MTs, and the average staining density can be reflected by the average digitized gray values. The normalized average gray values were measured as a function of horizontal position in the cells, integrated in the vertical direction, and plotted as a summed histogram. Fig. 6 is typical of these measurements and shows that there is no synchronous regrowth or shrinkage of the transected MTs. Cells fixed and stained 20 s after laser transection showed 10-μm-wide troughs in the transected zones in the summed histograms (Fig. 6, $T = 20$ *s*), indicating the depletion of MTs in those regions. With time the troughs gradually shallowed, indicating an increase in the number of MTs in those regions. This is contrary to the two predictions of the treadmilling model (Fig. 1, *A* and *B*), which in this case would predict that with time the trough would either remain unchanged or

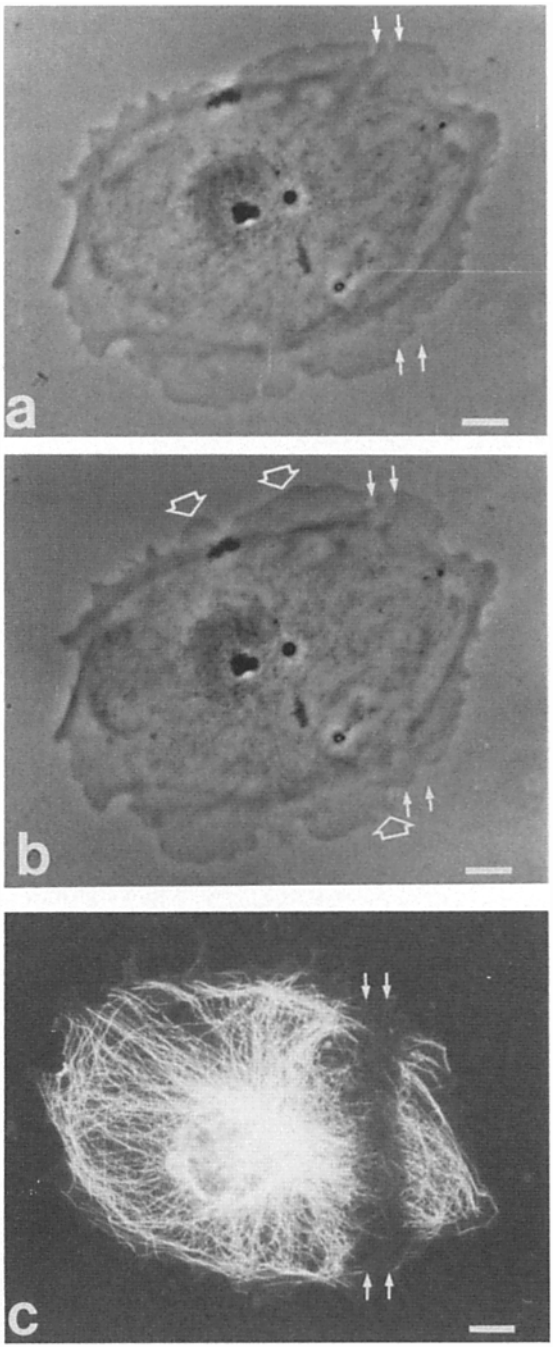

Figure 4. Effects of laser irradiation on cell morphology. Phase-contrast micrographs of a PtK_2 cell (*a*) before and (*b*) 2 min after irradiation. Open arrows in *b* depict the morphological changes that occurred after irradiation. The corresponding tubulin staining of the same cell fixed 10 min after irradiation (*c*) shows the transection of MTs. The predefined regions were indicated by small arrows outside the cells. Bars, 10 μm.

get narrower. On the other hand, such behavior of the MTs can be explained by dynamic instability.

Transected MTs With Free New Ends Do Not Quickly Disappear

Another result from the above experiments is that the majority of MTs with free new ends generated by in situ laser transection do not immediately depolymerize to completion, and the free minus ends of these MTs are relatively stable. If shrinking MTs rapidly disassemble to completion and the free minus ends of these MTs were unstable, a drastic decrease in the number of MTs in regions proximal from transected zones in relation to the cell nuclei, and a total lack of MTs in regions distal from transected zones soon after the transection would be expected because transecting the internal regions of MTs would result in all the transected MTs entering the shrinking phase. Fig. 5, *b–d*, along with Fig. 4 *c*, shows that most transected MTs do not disappear for periods of more than 10 min, and there is no drastic decrease in the number of MTs or MT density on both sides of transected zones, indicating that most transected MTs do not rapidly depolymerize to completion. This is more obvious for the MTs with free minus ends, and some of the free minus ends can be detected in cells fixed 19 min after transection (Fig. 5 *d*).

Quantitative Analyses of Transected MTs

To further confirm the above results, we have examined negatives for 84 cells and quantitated the number of MTs both in transected zones and in regions on the distal side (toward the leading edges of the cells) of the transected zones as a function of time. Although the cells selected for this study had similar size and morphology, relatively small variations in cell sizes and in MT density were observed. The variations in cell sizes were overcome by converting the number of MTs to MT density, and variability in MT density was estimated by conducting the same measurements on untreated cells. To facilitate tracking of individual MTs, the immunofluorescent images were digitized and processed as described in Materials and Methods. The digital processing enhanced the contrast in MT and nonMT regions. Individual MTs in regions from several micrometers away from the side of a transected zone in proximity to the nucleus all the way to the cell leading edge can be readily tracked on the video monitor. Fig. 7 confirms that the number of MTs in transected zones increases progressively with time and that by ~30 min after transection of MTs, the laser-dissociated MTs are completely replaced by newly grown MTs; consequently, the half-time of such a replacement is calculated to be ~10 min. When quantitating the number of MTs in the regions between the transected zones and cell edges, however, we have again found that most transected MTs do not catastrophically disassemble and these MTs which have free new minus ends persisted, although the number of MTs slightly decreases at the beginning (20 s to 7 min) and then increases with time in comparison with control cells (Fig. 8).

Discussion

We have developed a new approach to study the mechanism of cytoplasmic MT turnover by combining laser microsurgery with immunocytochemistry. This method avoids some of the possible drawbacks of other techniques such as an increase in intracellular tubulin concentration and total cell volume. The data presented here show that the majority of cytoplasmic MTs in interphase cells exhibit individuality of growth and shrinkage after transection of the MTs, and the half-time of complete MT replacement after laser transection

is estimated to be ~10 min, compatible with other in vivo and in vitro studies of end-dependent MT assembly (17, 37–39). Simultaneous growth or shrinkage of all MTs was never observed under the experimental conditions. These results are contrary to the predictions of the treadmilling model, and suggest that a majority of cytoplasmic MTs in cultured cells exhibit some properties of dynamic instability (individual regrowth and shrinkage). On the other hand, our results also show that the exposure of the core of the MTs, which is expected to consist almost completely of GDP-tubulin subunits according to the GTP cap model, by transecting the internal regions of the MTs does not render the remaining polymer catastrophically disassembled, and most transected MTs with exposed free minus ends do not quickly disappear. This is not in agreement with the predictions of GTP cap model, and suggests that under in vivo conditions, other factors in addition to the hydrolysis of GTP need to be involved in modulating the dynamics and stability of these dynamic cytoplasmic MTs.

It has been demonstrated that MT-associated proteins bind to the outside surface of MTs, altering the energetics and kinetics of their assembly and disassembly. In addition, certain divalent cations such as Mg^{2+} and Ca^{2+}, etc., have been shown to affect MT assembly and disassembly. Based on the fact that most transected MTs with free new ends in PtK_2 cells do not quickly disappear, we propose that in vivo the hydrolysis of GTP-tubulin may not cause a rapid disassembly. Rather it would change the interactions between the subunits in the polymer only to such a degree as to permit the GDP polymer to exist in a metastable state. This structurally stable GDP polymer may then be further stabilized or induced to rapidly disassemble by other factors such as MT-associated proteins, and Ca^{2+} etc., and it may exchange with either free GDP-tubulin or free GTP-tubulin at an MT end with different rates. Under certain conditions, more than one kind of factor may simultaneously act on MTs, and some of them may even act randomly. One recent study has also suggested the presence of factors in Madin–Darby canine kidney cells which stabilize the noncentrosomal cytoplasmic MTs (4). These factors may play important functional roles in modulating the dynamics and stability of MTs in vivo. Although the hypothesis discussed above can well explain the stability of MTs with exposed free ends in cells, the possibility could exist that the laser somehow "cauterized" the transected MT ends so that they were no longer reactive. However, the following observations argue against this possibility: (*a*) the laser-dissociated MTs are completely replaced, and the time course of such replacement is compatible with other in vivo and in vitro studies of MT assembly using different methodologies; and (*b*) irradiated cells incubated at 4°C for periods of 15–30 min show a complete loss of fibrillar MT staining even in the irradiated regions, suggesting that the MT ends are able to undergo a net loss of tubulin subunits under depolymerizing conditions.

The observed replacement of laser-dissociated MTs in the transected zone is unlikely to be explained by some form of active sliding of the MTs. First, if the transected MTs actively slid into the transected zone, then a number of short MTs with both ends free would be present in regions around the transected zone soon after the transection, and these short MTs would be accumulated with time while the transected zone gradually refilled with MTs. However, when we performed our quantitative analyses, individual MTs in regions around the transected zones were traced from a video monitor after computer enhancement, and no such short MTs with both ends free were found. Second, the observed time course of replacement of laser-dissociated MTs in the transected zone is much too slow to be explained by the active sliding of MTs. As our data showed, it took about 30 min to completely refill the 10-μm-wide transected zone with MTs; but, the reported rate of active sliding of MTs of the same polarity ranges from 0.2–16 $\mu m/s^{-1}$ (21, 29, 32, 33, 35, 43). Apparently, the expected time course of refill of the MT-depleted zone by some form of active sliding of the MTs would be much faster than the observed time course, even when the lowest reported rate of MT sliding is considered.

It is necessary to emphasize that our results may be limited to cultured interphase cells whose MTs are dynamic and undergoing constant remodeling. It is known that MTs in some terminally differentiated cells, such as neurons and mature chicken erythrocytes, have distinct properties which differ from those of MTs in cultured cells. These MTs are more stable and lack MT organizing centers (6, 19). In these cases, the stability and possible lateral interactions of MTs appear to be more important than the dynamic aspects of MTs in order for the MTs to perform their functions. Different mechanisms may be needed to be involved to achieve such stability and spatial organization.

In mammals, the α and β tubulins are encoded by multigene families (reviewed in reference 8), and it seems that more than one gene for the tubulins are expressed in any cell type at any time, which results in the presence of multiple tubulin isotypes in a cell. The existence of different tubulin isotypes led to speculation that distinct kinds of MTs might be assembled from or enriched in one or more tubulin isotypes (12). Therefore, it raises the possibility that there might exist subsets of MTs with different properties in cultured cells due to the structural difference in isotype contents. However, very recent studies have demonstrated that in cultured cells these isotypes form mixed copolymers and appear to function interchangeably (3, 24). It has been shown that the coexistence of two populations of MTs in cells with different stabilities which could probably result from post-translational modification(s) or binding of MT-associated proteins along their length is possible. However, not only do the dynamic MTs represent 80% of all MTs while stable MTs only represent 20% but also the overall shapes and spatial distributions of these two populations are quite different from one another. The stable MTs are curly or kinky, compared to the dynamic MTs which are usually straight and cluster around the nucleus and centrosome. In addition, the stable MTs rarely extend to the cell periphery, as opposed to the dynamic MTs many of which reach the cell's edge (4, 13, 39). Since the transected zones chosen for this study are located relatively far away from the nuclei, the stable MTs which would be found within the transected zones represent a very small fraction of all the MTs in those regions. Therefore, any possible diversity in MT assembly resulting from the coexistence of stable and dynamic populations of MTs would make a very small contribution to the observed MT behavior after laser transection in situ. It is possible that mechanisms for the turnover of such a small percent of stable MTs may be different from that for the turnover of dynamic MTs. It is not surprising, however, if we come to think these

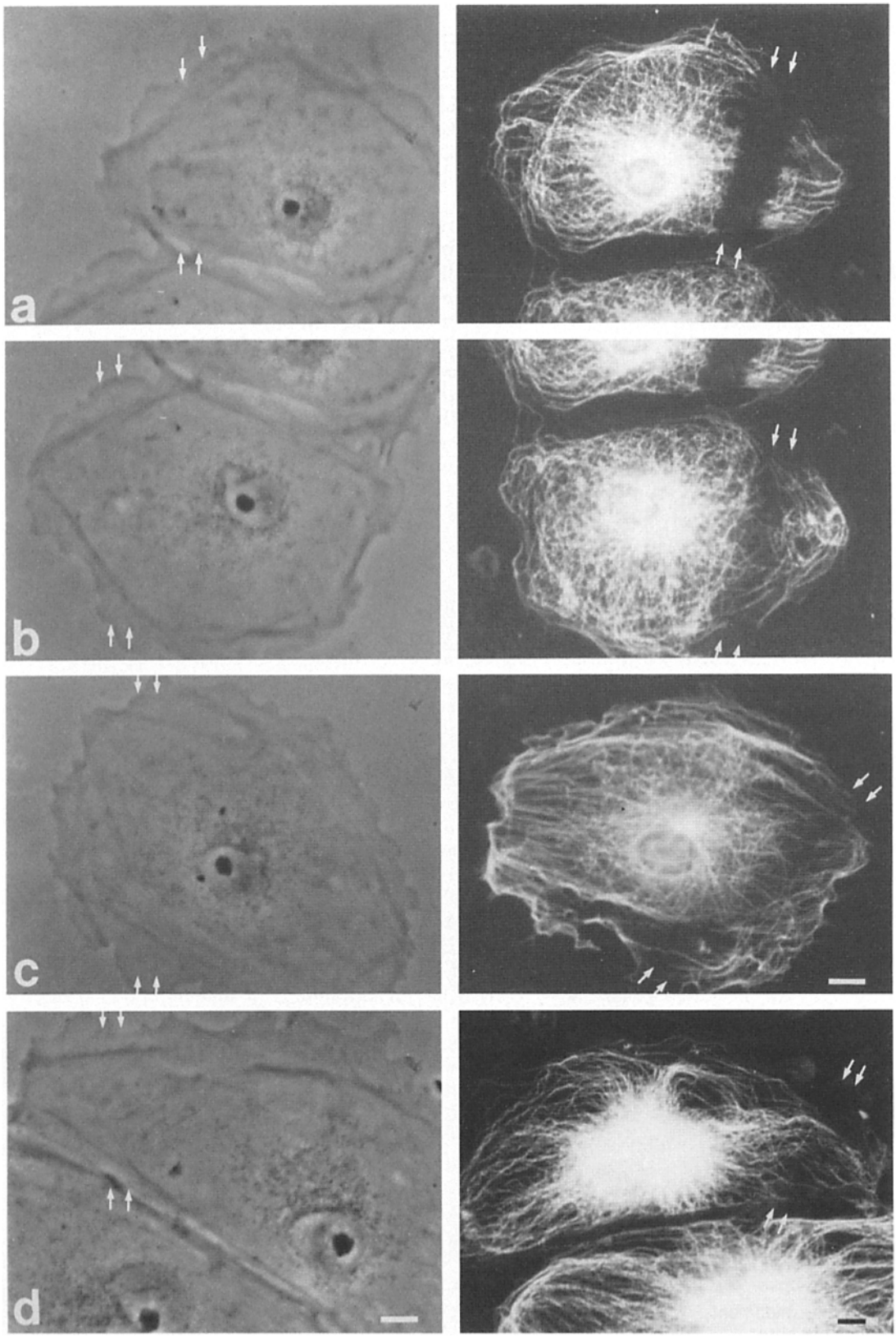
a
b
c
d

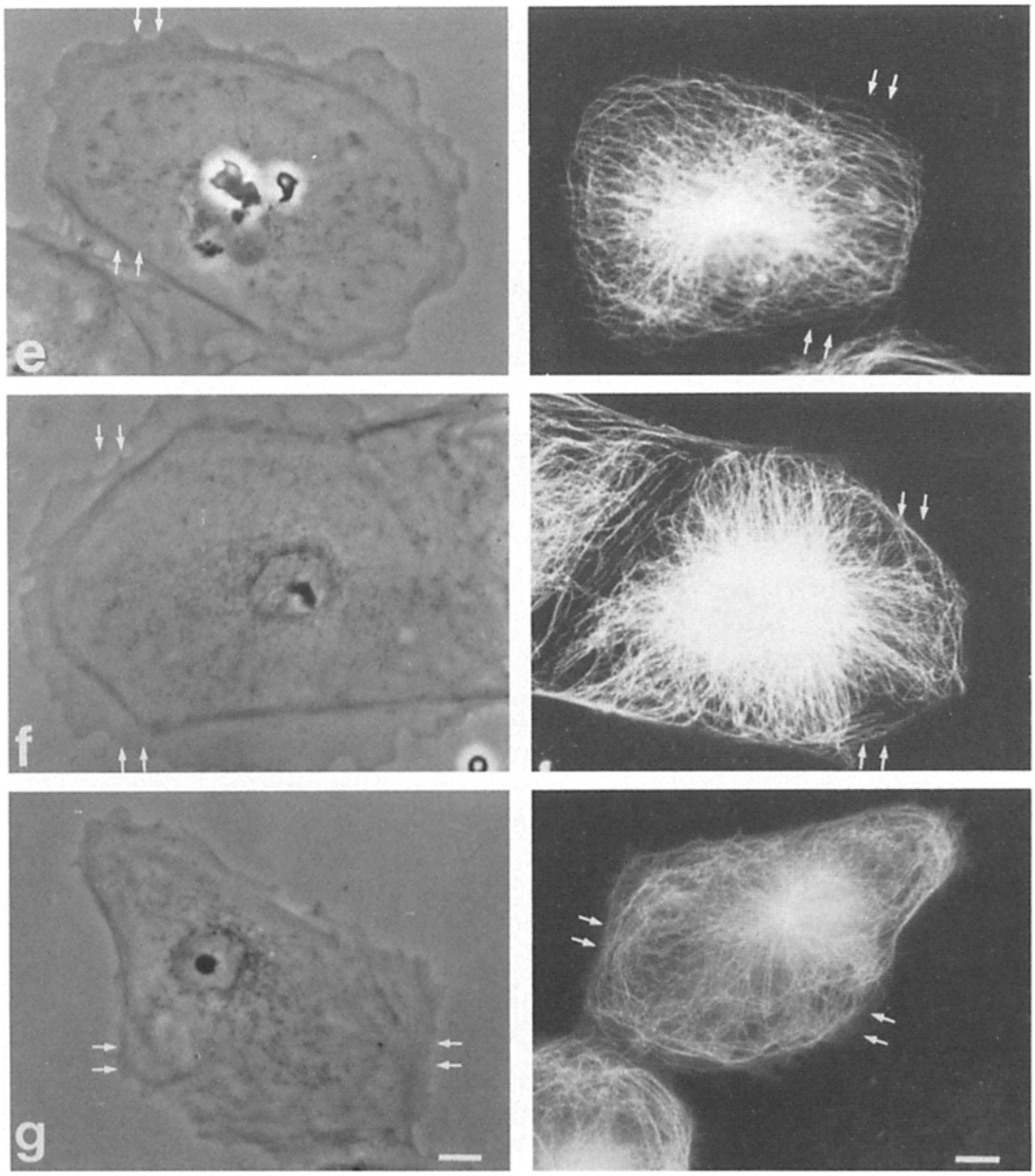

Figure 5. Regrowth of MTs after transection. Phase contrast and corresponding antitubulin fluorescence of cells whose MTs were laser dissociated in the transected zones. *Arrows*, predefined regions. The cells (fluorescent micrographs) were fixed 20 s and 9, 13, 19, 28, 35, and 55 min after laser transection, respectively, and then stained with antitubulin mAb. Bars, 10 μm.

MTs may have specialized functions and be involved in such diverse processes as intracellular transport or sensing of environmental changes coupled with communication of the signal to the nucleus.

At present, the exact identities of the factors that regulate the dynamics and stability of MTs in vivo and the molecular mechanism by which they would function are still unclear. Elucidation of these factors is fundamental to achieving a better understanding of cell function.

We would like to thank Drs. E. D. Salmon and C. L. Rieder for stimulating discussion and helpful suggestions. We are also grateful to Drs. Frank Solomon and James Aist for their helpful comments on the manuscript.

This work was supported by National Institutes of Health grants RR-01192 and CA-32248, and by a grant from the Office of Naval Research (N 00014-86-K-0115).

Received for publication 25 April 1988.

References

1. Bergen, L., R. Kuriyama, and G. G. Borisy. 1980. Polarity of microtubules nucleated by centrosomes and chromosomes of Chinese hamster ovary cells in vitro. *J. Cell Biol.* 84:151–159.
2. Berns, M. W., J. Aist, J. Edwards, K. Strahs, J. Girton, M. Kitzes, M. Hammer-Wilson, L. H. Liaw, A. Siemens, M. Koonce, S. Peterson, S. Brenner, J. Burt, R. Walter, P. J. Bryant, D. Dyk Van, J. Coulombe, T. Cahill, and G. S. Berns. 1981. Laser microsurgery in cell and developmental biology. *Science (Wash. DC).* 213:505–513.
3. Bond, J. F., J. L. Fridovich-Keil, L. Pillus, R. C. Mulligan, and F. Solomon. 1986. A chicken-yeast chimeric β-tubulin protein is incorporated into mouse microtubules in vivo. *Cell.* 44:461–468.
4. Bre, M.-H., T. E. Kreis, and E. Karsenti. 1987. Control of microtubule nucleation and stability in Madin–Darby canine kidney cells: the occurrence of noncentrosomal, stable detyrosinated microtubules. *J. Cell Biol.* 105:1283–1296.

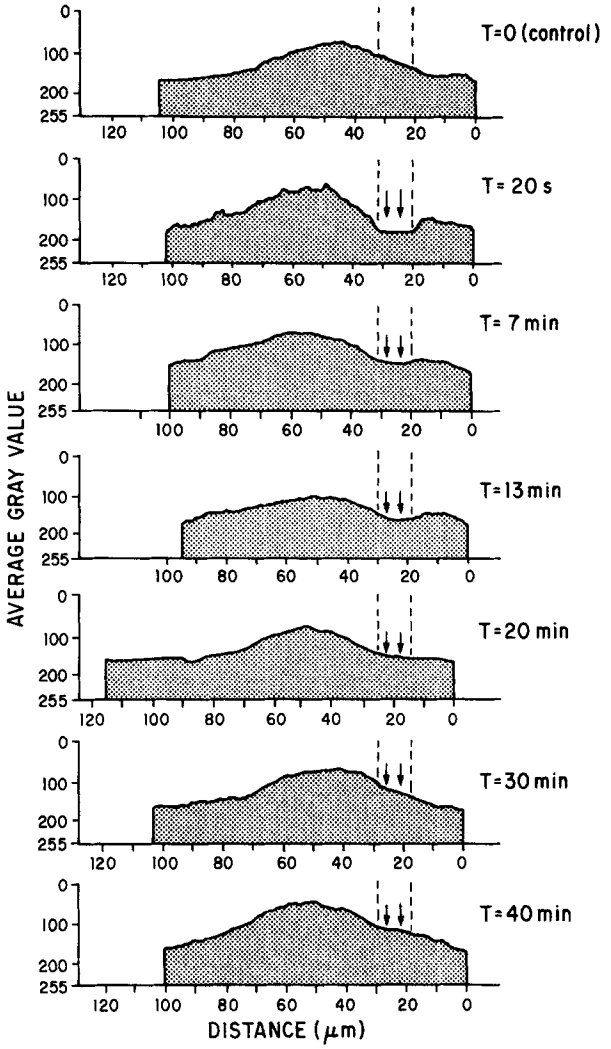

Figure 6. Average properties of the MT behavior as a function of time. The distributions of measured average gray values in each histogram correspond to the average variations in MT staining in the digital image of a cell. Distance was measured from one side of a cell edge to the other. *Arrows*, predefined regions; *dashed lines*, the actual transected zones on the fluorescence micrographs. *T*, the time intervals between irradiation and fixation; $T = 0$, untreated control cells.

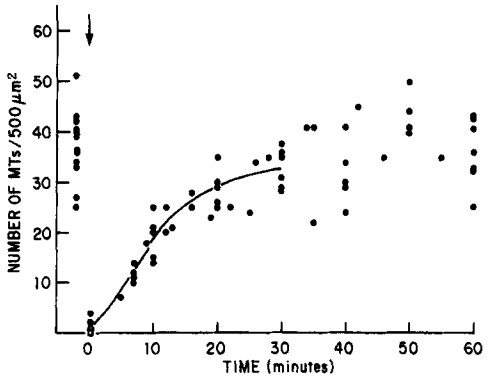

Figure 7. Increase in the number of MTs in transected zones with time. The MT density in both control cells (on the left side of the arrow) and experimental cells (on the right side of the arrow) was measured. The data points are collected from one (*solid circle*), six (*open triangle*), and nine cells (*open square*), respectively. *Arrow*, the time at which MTs were transected in situ.

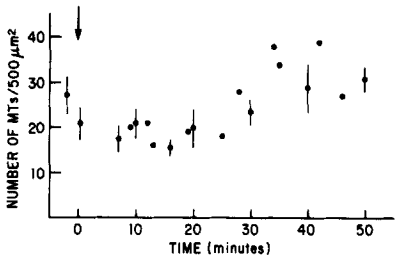

Figure 8. Quantification of MTs in regions distal from the transected zones. The MT density in both control cells (on the left side of the arrow) and experimental cells (on the right side of the arrow) was measured. *Arrow*, the time at which MTs were transected in situ. *Solid circles*, data from single cells; *error bars*, SDs.

5. Cassimeris, L. U., P. Wadsworth, and E. D. Salmon. 1986. Dynamics of microtubule depolymerization in monocytes. *J. Cell Biol.* 102:2023-2032.
6. Chalfie, M., and J. Thompson. 1979. Organization of neuronal microtubules in the nematode *Caenorhabditis elegans*. *J. Cell Biol.* 82:278-291.
7. Chen, Y.-D., and T. L. Hill. 1985. Theoretical treatment of microtubules disappearing in solution. *Proc. Natl. Acad. Sci. USA.* 82:4127-4131.
8. Cleveland, D. W., and K. F. Sullivan. 1985. Molecular biology and genetics of tubulin. *Annu. Rev. Biochem.* 54:331-365.
9. Cote, R. H., and G. G. Borisy. 1981. Head to tail polymerization of microtubules in vitro. *J. Mol. Biol.* 150:577-602.
10. Dustin, P. 1984. Microtubules. Springer-Verlag New York, Inc., New York. 482 pp.
11. Euteneuer, U., and J. R. McIntosh. 1981. Structural polarity of kinetochore microtubules in PtK1 cells. *J. Cell Biol.* 89:338-345.
12. Fulton, C., and P. A. Simpson. 1976. Selective synthesis and utilization of flagellar tubulin: the multitubulin hypothesis. *Cell Motil.* 3:987-1005.
13. Gundersen, G., M. H. Kalnoski, and J. C. Bulinski. 1984. Distinct populations of microtubules: tyrosinated and nontyrosinated alpha tubulin are distributed differently in vivo. *Cell.* 38:779-789.
14. Haimo, L. T., B. R. Telzer, and J. L. Rosenbaum. 1979. Dynein binds to and crossbridges cytoplasmic microtubules. *Proc. Natl. Acad. Sci. USA.* 76:5759-5763.
15. Hill, T. L., and M.-F. Carlier. 1983. Steady-state theory of the interference of GTP hydrolysis in the mechanism of microtubule assembly. *Proc. Natl. Acad. Sci. USA.* 80:7234-7238.
16. Hill, T. L., and Y.-D. Chen. 1984. Phase changes at the end of a microtubule with a GTP cap. *Proc. Natl. Acad. Sci. USA.* 81:5772-5776.
17. Horio, T., and H. Hotani. 1986. Visualization of the dynamic instability of individual microtubules by dark-field microscopy. *Nature (Lond.).* 321:605-607.
18. Johnson, K. A., and G. G. Borisy. 1977. Kinetic analysis of microtubule self-assembly in vitro. *J. Mol. Biol.* 117:1-131.
19. Kim, S., M. Magendantz, W. Katz, and F. Solomon. 1987. Development of a differentiated microtubule structure: formation of the chicken erythrocyte marginal band in vivo. *J. Cell Biol.* 104:51-59.
20. Kirschner, M. 1980. Implications of treadmilling for the stability and polarity of actin and tubulin polymers in vitro. *J. Cell Biol.* 86:330-334.
21. Koonce, M. P., J. Tong, U. Euteneuer, and M. Schliwa. 1987. Active sliding between cytoplasmic microtubules. *Nature (Lond.).* 328:737-739.
22. Koshland, D. E., T. Mitchison, and M. Kirschner. 1988. Polewards chromosome movement driven by microtubule depolymerization in vitro. *Nature (Lond.).* 331:499-504.
23. Kristofferson, D., T. Mitchison, and M. Kirschner. 1986. Direct visualization of steady-state microtubule dynamics. *J. Cell Biol.* 102:1007-1019.
24. Lewis, S. A., W. Gu, and N. J. Cowan. 1987. Free intermingling of mammalian β-tubulin isotypes among functionally distinct microtubules. *Cell.* 49:539-548.
25. Margolis, R. L., and L. Wilson. 1978. Opposite end assembly and disassembly of microtubules at steady state in vitro. *Cell.* 13:1-8.
26. Margolis, R. L., and L. Wilson. 1981. Microtubule treadmills—possible molecular machinery. *Nature (Lond.).* 293:705-711.
27. Mitchison, T., and M. Kirschner. 1984. Microtubule assembly nucleated by isolated centrosomes. *Nature (Lond.).* 312:232-237.
28. Mitchison, T., and M. Kirschner. 1984. Dynamic instability of microtubule growth. *Nature (Lond.).* 312:237-242.
29. Okagaki, T., and R. Kamiya. 1986. Microtubule sliding in mutant *Chlamydomonas* axonemes devoid of outer or inner dynein arms. *J. Cell Biol.* 103:1895-1902.
30. Oosawa, F., and S. Asakura. 1975. Thermodynamics of the polymerization of protein. Academic Press, New York. 194 pp.
31. Osborn, M., and K. Weber. 1976. Cytoplasmic microtubules in tissue culture cells appear to grow from an organizing structure towards the plasma membrane. *Proc. Natl. Acad. Sci. USA.* 73:867-871.

32. Paschal, B. M., S. M. King, A. G. Moss, C. A. Collins, R. B. Vallee, and G. B. Witman. 1987. Isolated flagellar outer arm dynein translocates brain microtubules in vitro. *Nature (Lond.).* 330:672–674.
33. Paschal, B. M., H. S. Shpetner, and R. B. Vallee. 1987. MAP 1C is a microtubule-activated ATPase which translocates microtubules in vitro and has dynein like properties. *J. Cell Biol.* 105:1273–1282.
34. Roberts, K., and J. S. Hyams. 1979. Microtubules. Academic Press, New York. 595 pp.
35. Sale, W. S. 1986. The axonemal axis and Ca^{2+}-induced asymmetry of active microtubule sliding in sea urchin sperm tails. *J. Cell Biol.* 102:2042–2052.
36. Salmon, E. D., R. J. Leslie, W. M. Saxton, M. L. Karow, and J. R. McIntosh. 1984. Spindle microtubule dynamics in sea urchin embryos: analysis using a fluorescent-labeled tubulin and measurement of fluorescence redistribution after laser photobleaching. *J. Cell Biol.* 99:2165–2174.
37. Sammak, P. J., G. J. Gorbsky, and G. G. Borisy. 1987. Microtubule dynamics in vivo: a test of mechanisms of turnover. *J. Cell Biol.* 104:395–405.
38. Schulze, E., and M. Kirschner. 1986. Microtubule dynamics in interphase cells. *J. Cell Biol.* 102:1020–1031.
39. Schulze, E., and M. Kirschner. 1987. Dynamic and stable populations of microtubules in cells. *J. Cell Biol.* 104:277–288.
40. Soltys, B. J., and G. G. Borisy. 1985. Polymerization of tubulin in vivo: direct evidence for assembly onto microtubule ends and form centrosomes. *J. Cell Biol.* 100:1682–1689.
41. Srinivason, R. 1986. Ablation of polymers and biological tissue by ultraviolet lasers. *Science (Wash. DC).* 234:559–565.
42. Tao, W., J. Wilkinson, E. J. Stanbridge, and M. W. Berns. 1987. Direct gene transfer into human cultured cells facilitated by laser micropuncture of the cell membrane. *Proc. Natl. Acad. Sci. USA.* 84:4180–4184.
43. Vale, R. D., T. S. Reese, and M. P. Sheetz. 1985. Identification of a novel force generating protein, kinesin, involved in microtubule-based motility. *Cell.* 42:39–50.
44. Water, R. J., and M. W. Berns. 1981. Computer-enhanced video microscopy: images can be produced in real time. *Proc. Natl. Acad. Sci. USA.* 78:6927–6931.